Advancements on the use of the Non Local Means algorithm for seismic data processing

Carlo De Gaetani, Samuel Winters, Sergio Grion, Dolphin Geophysical Ltd.*

Summary

Among the techniques and algorithms usually applied to seismic data for random noise attenuation, Non Local Means (NLM) filtering is a promising option. It is based on a weighted mean in which the weights depend on the measure of similarity between patches surrounding each sample. This methodology allows the preservation of features and structures while incoherent signal is filtered out. The application of such methodology can be n-dimensional but its high computational cost disadvantages a 3D implementation. In previous work we presented a revised version of the NLM algorithm, improved from both the computational and signal to noise enhancement points of view. In the present paper we focus on the application of this revised NLM on real data time-slices, and investigate more in detail the 3D implementation of the method.

Introduction

Originally, Buades et al. (2005) developed the Non Local Means (NLM) algorithm for digital image processing but the capability of separating coherent and incoherent signal and of preserving features, edges and structures has made it popular for many other applications. Bonar and Sacchi (2012) introduce the NLM for seismic data processing purposes, proving the effectiveness of such algorithm in comparison with more standard techniques for noise attenuation like *f-x* deconvolution. Maraschini and Turton (2013) present a windowed variant of the NLM, in order to reduce the requested high computational cost and propose a time-variant harshness of the filtering for applications on time-slices. De Gaetani et al. (2016) further investigate several aspects of the NLM, like the use of different convolutional kernels, anisotropy and asymmetry of the search window and the comparison patch, the weight to be assigned to the reference patch and the 3D extension of the algorithm. The achievements of this revised version of the NLM show a combination of computational simplification and better results in terms of signal to noise ratio enhancement.

In this paper we present the continuation of those analyses. We focus on the application to time-slices of a 3D cube and on the improvements obtainable with this 3D application.

Method

In this section we give a brief description of our revised NLM. A more detailed description of the key points investigated can be found in De Gaetani et al. (2016).

If $v(i)$ is the amplitude of sample i and $v(j)$ the amplitude of one of m samples j not necessarily in the vicinity of i, a filtered value $\hat{v}(i)$ is obtained with the weighted mean:

$$\hat{v}(i) = \frac{\sum_j w\,(i,j)v(j)}{\sum_j w\,(i,j)}$$

where the weights:

$$w(i,j) = exp\left(\frac{-D^2(i,j)}{h^2}\right)$$

depend on the measure of relative distance $D(i,j)$ between the sample i and the windowed m samples j and an harshness parameter h. The distance

$$D(i,j) = K \cdot \left(v(N_i) - v(N_j)\right)$$

is computed evaluating the similarity between the neighborhood patches N_i and N_j surrounding the samples i and j respectively and balanced by a convolutional kernel K.

The main issue with this algorithm is its complexity, which depends on the dimension of the patches and of the window search, and, in practice, limits its application. This limit can be properly addressed by changing the shape of the kernel (from Gaussian to uniform) and the size of the search window and patches (depending on the target features). Furthermore, the capability of the algorithm to increase the signal to noise ratio of seismic images can be improved assigning to the reference patch a weight $w_{ii} = max(w_{ij})$.

In the following section we present examples of the advancements brought forward by our revised NLM and we discuss the 3D extension of the algorithm.

Advancements on the use of the NLM algorithm

Examples

First, we present the main achievements obtainable with our revised NLM algorithm. We compare the use of different kernels and the impact of weighting the reference patches properly by applying the NLM to a time-slice (t=1500ms) of a 3D pre-migration common-offset (135m) volume. On this time-slice there is no reason for targeting particular directions, therefore we use square patches and square windows. The input time-slice is shown in figure 1 and a summary of the tests carried out is presented in table 1 where patch size is defined as in-line x cross-line samples.

	$w(i,i)$	kernel	patch size
Test A	1	Gaussian	19x19
Test B	1	uniform	7x7
Test C	1	uniform	7x7
Test D	$\max(w(i,j))$	uniform	7x7

Table 1: NLM parameters, tests on kernel and $w(i,i)$.

We comment the results analyzing the difference between the input and the filtered data, rescaled by a factor 10 for better visualization. For all tests, parameter h is set to 1.5 and the search window size is 7x7 (in-line and cross-line, respectively). We choose to comment in detail results from areas 1 and 2 in figure 1.

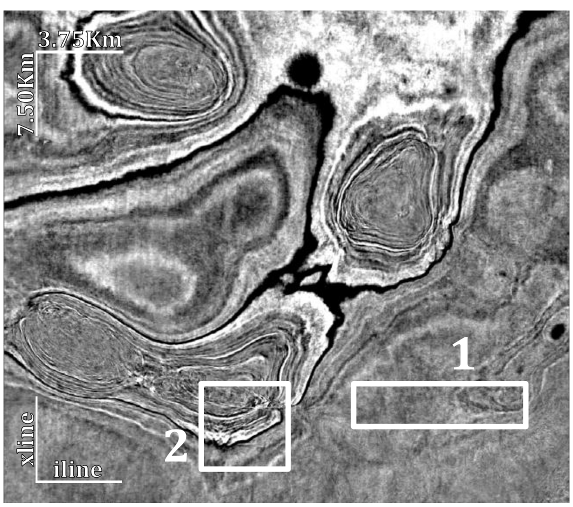

Figure 1: Time-slice before applying NLM and analyzed areas.

Area 1 contains weak signal while area 2 contains stronger signal. Using data from area 1 it is then possible to check if, changing the convolutional kernel, the amount of noise detected and removed is comparable. We show the result of the noise detection obtained in tests A and B in figure 2.

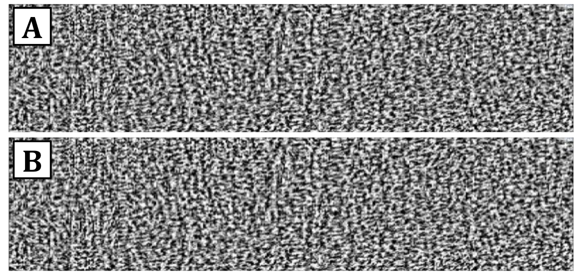

Figure 2: Noise detected in area 1 by tests A and B.

Using either a Gaussian or a uniform kernel gives equivalent results. This is also confirmed by inspection of the power spectra of the detected noise from area 1 for both tests, shown in figure 3.

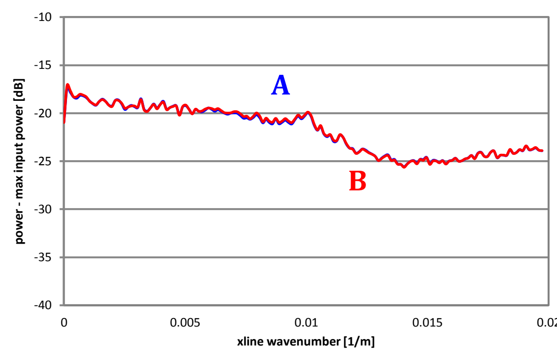

Figure 3: Power spectra of noise detected in area 1.

While results are comparable, a substantial efficiency improvement comes from the reduced patch size when a uniform kernel is used. The complexity of the algorithm in test B is about 7.3 times less than in test A without any loss in noise removal capability. Both tests preserved coherent signal, as demonstrated by the absence of coherent energy in the difference sections of figure 2.

Area 2 is a part of the time-slice in which the signal of interest is particularly difficult to preserve. In this area there are quick changes of amplitude polarity and curved and faulted edges that must be protected from the noise removal process. This portion of the data is therefore suitable for assessing the impact of changing the reference patch weight definition. When $w(i,i)$ is computed sliding the comparison patch N_j exactly over the reference patch N_i, the weight assigned has a value of 1. The NLM algorithm then gives to the central sample of the window an unbalanced weight with respect to the others, and leaves it almost untouched. This is clear looking at the differences between the input and the filtered data, shown in figure 4 where noise detected by test C and D is displayed.

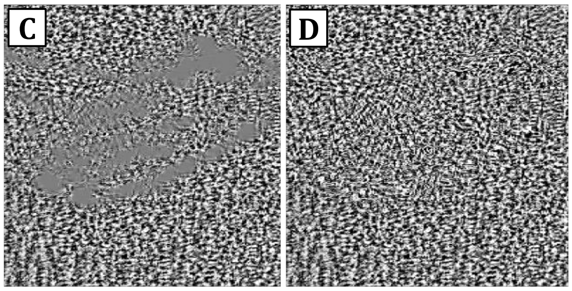

Figure 4: Noise detected in area 2 by tests C and D.

In figure 4, small differences obtained by test C mean minimal noise removal, and they correspond to those areas in which the NLM detects the presence of edges and features. In test D the result is definitely different. The noise detection is homogeneous and noise is removed also when it overlaps the signal of interest. In figure 5 we show the power spectra of the noise detected from tests C and D. As we can see, the noise content revealed in test C is definitely less than in test D.

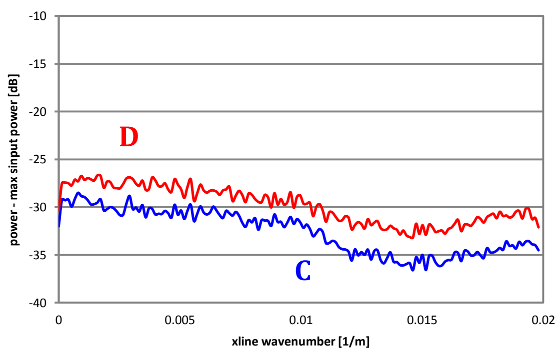

Figure 5: Power spectra of noise detected in area 2.

We now carry out a similar analysis to investigate 3D patches and 3D windows. Table 2 (in which the patch and window sizes are intended as in-line x cross-line x time samples) summarizes these tests.

	patch size	window size
Test E	7x7x1	7x7x1
Test F	7x7x3	7x7x1
Test G	7x7x1	7x7x3
Test H	7x7x3	7x7x3

Table 2: NLM parameters, tests on 3D extension.

Similarly to the previous tests, the h parameter has a value of 1.5. We use a uniform kernel and the weight of the reference patch is defined as $w(i,i) = \max(w(i,j))$. We comment the results referring again to the difference between the input and the filtered data, rescaled by a factor of 10, focusing on areas 1 and 2 (of figure 1. In figure 6 we show the noise detected by NLM with the tested parameterizations for area 1.

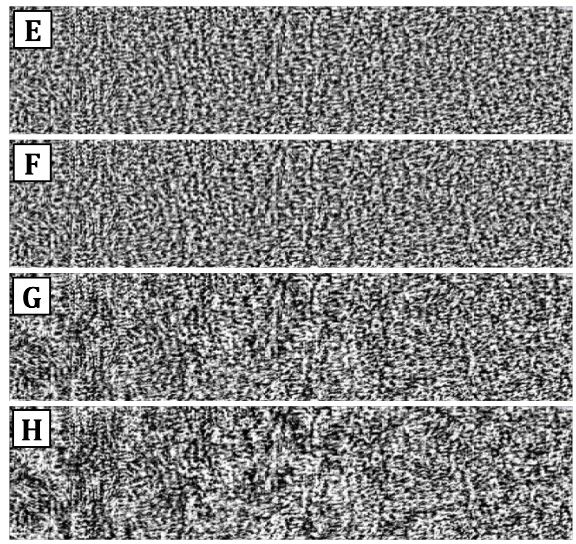

Figure 6: Noise detected in area 1 by tests E, F, G and H.

In test E both the patches and the window search are 2D and increasing the thickness of the comparison patches (test F) does not produce significant additional noise reduction. The main difference occurs when a 3D window search is used as in test G and test H. In these cases the filtering results are harsher, in particular when a combination of 3D patches and windows are used (test H). In figure 7 the power spectra of the four close-ups just described are displayed. From test E to test H, the power spectra increase and corresponds to an increase in the amount of noise detected and removed by the algorithm.

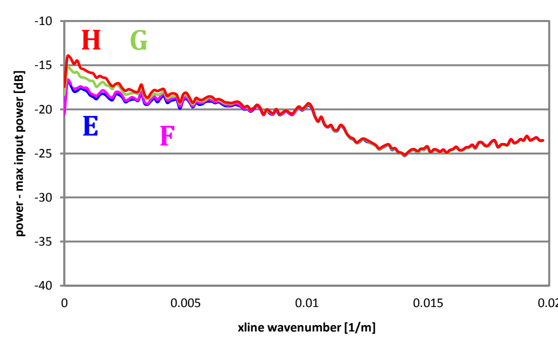

Figure 7: Power spectra of noise detected in area 1.

The complexity of the algorithm increases when the 3D extension is considered and this point needs to be taken into account. Both test F and test G have a complexity three times bigger than the 2D case (test E) but test G obtains a significant better result. Results obtained in area 2 are quite similar. We show the noise detection of the test series in this area in figure 8.

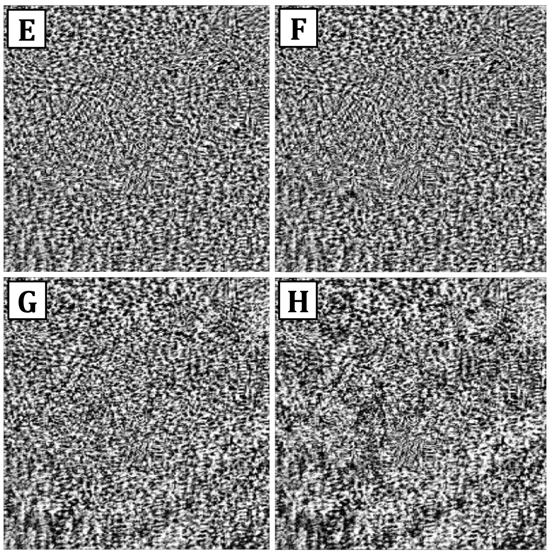

Figure 8: Noise detected in area 2 by tests E, F, G and H.

With respect to the standard 2D case (test E), using 3D patches and 2D windows does not produce significant improvements in terms of noise removal and the power spectra of these tests are almost identical (see figure 9). The only difference between test E and test F is in the increased complexity of the algorithm. Again, it is the 3D extension of the search window that brings improvements. The filtering process becomes harsher and the signal component remains preserved but, as previously mentioned, with a substantial increase in computational cost.

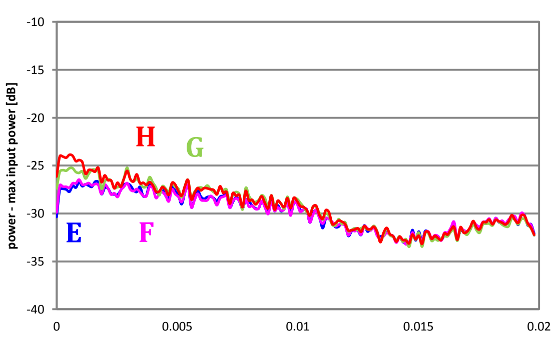

Figure 9: Power spectra of noise detected in area 2.

In figures 10 and 11 we show the close-up on area 1 and area 2 of the initial and the filtered time-slice obtained with test G, the best compromise between quality of the result and computational cost.

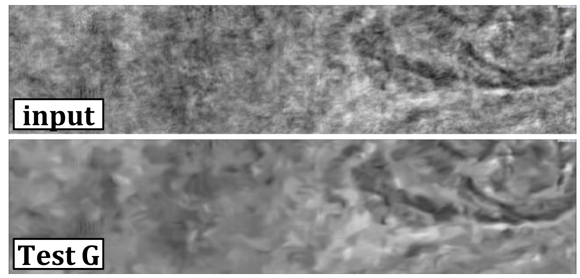

Figure 10: Area 1, input and filtered data.

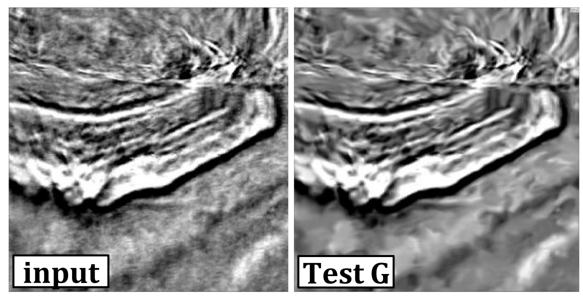

Figure 11: Area 2, input and filtered data.

Conclusion

Our analyses on time-slices of a real 3D volume prove the effectiveness of our revised NLM algorithm in seismic data processing applications. The use of a uniform kernel instead of a Gaussian diminishes the complexity of the algorithm without losing noise detection capability. Additionally, with a proper weighting of the reference patch the reduction of incoherent noise improves and features and edges are better preserved. Signal to noise ratio enhancement does not benefit from the extension of the comparison patches to 3D while improvements are obtained when the search window is extended. However, the improvements in terms of quality of the noise attenuation are counterbalanced by an increment of the computational cost that must be taken into account.

Acknowledgements

We thank Dolphin Geophysical Multi Client department for the permission to publish our tests carried out on real data.

References

Bonar, D., and M. Sacchi, 2012, Denoising seismic data using the Nonlocal means algorithm: Geophysics, 77, no. 1, A5-A8, doi: 10.1190/GEO2011-0235.1.

Buades, A., B. Coll and J.M. Morel, 2005, A review of image denoising algorithms, with a new one: SIAM Journal on multiscale modeling and simulation, 70, no. 2, 490-530, doi: 10.1137/040616024.

De Gaetani, C., J. Barnes, S. Winters and S. Grion, 2016, Practical aspects of Non Local Means filtering of seismic data: 78th Conference & Exhibition, EAGE, Extended Abstracts, Th STZ1 02.

Maraschini, M., and N. Turton, 2013, Random noise attenuation preserving geological detail – A fast and effective Non-Local-Means filter: 75th Conference & Exhibition, EAGE, Extended Abstracts, doi: 10.3997/2214-4609.20130881.